#247

OGO-5

PLASMA SPECTROMETER HOURLY AVERAGES

68-014A-17B

OGO 5

HR AVG PLASMA PARAM ON TAPE

68-014A-17B

THIS DATA SET HAS BEEN RESTORED. THE ORIGINAL TAPES WERE 9-TRACK, 800 BPI, WITH ONE FILE OF DATA EACH AND WRITTEN IN BCD. THERE IS ONE RESTORED TAPE WRITTEN IN ASCII. THE DR TAPE IS A 3480 CARTRIDGE AND THE DS TAPE IS 9-TRACK, 6250 BPI. THE ORIGINAL TAPES WERE CREATED ON AN IBM 3081 COMPUTER AND THEY WERE RESTORED ON THE MRS SYSTEM. THE DR AND DS NUMBERS ALONG WITH THE CORRESPONDING D NUMBERS AND THE TIME SPAN IS AS FOLLOWS:

DR#	DS#	D#	FILES	TIME SPAN
DR02900	DS02900	D13102	1	03/05/68 - 04/30/71
		D29204	2	03/05/68 - 04/30/71

REQ. AGENT	RAND NO.	ACQ. AGENT
WTJ	RB4825	DJH

OGO-5

PLASMA SPECTROMETER HOURLY AVERAGES

68-014A-17B

This data set consists of 2 OGO-5 Hourly Averages Magnetic Tapes. This data tape, created on a IBM 7094 computer, is 7 track, 556 BPI, BCD and contains one file of data.

D#	C#	TIME SPAN
D-13102	C-09837	3/05/68 - 4/30/71

This data tape, created on a MODCOMP computer, is 9 track, 800 BPI, ASCII and contains one file of data.

D#	C#	TIME SPAN
D-29204	C-18799	3/05/68 - 4/30/71

68-014A-1 1D

PRODUCTION PROCESSING OF THE POSITIVE-ION SOLAR WIND DATA OBTAINED BY THE JPL OGO-5 PLASMA SPECTROMETER

Marcia Neugebauer and Barbara A. Weber
Jet Propulsion Laboratory
Pasadena, California 91103

March, 1973

ADDITIONAL DOCUMENTATION
B14068
COMPUTATION OF SOLAR WIND PARAMETERS FROM THE OGO-5 PLASMA SPECTROMETER DATA USING HERMITE POLYNOMIALS

TABLE OF CONTENTS

1. Instrumentation

2. Data Reduction

3. Spectrum-by-Spectrum Data

   A. Magnetic Tapes

   B. Listing

   C. Plots

4. Hourly-Average Data

   A. Punched Cards

   B. Listing

   C. Plots

5. Bibliography

   A. Papers specifically referred to in text.

   B. Other papers whose major purpose is the presentation or use of data from this experiment.

   C. Other papers which make some use of data from this experiment.

1. INSTRUMENTATION

The OGO-5 plasma experiment consisted of a Faraday-cup detector and a curved-plate analyzer which both pointed toward the sun at all times and an identical set of sensors which pointed radially away from the Earth. The instrumentation is described in detail in Reference 1.

The solar-wind data collected here were obtained by the solar-oriented set of instruments when the satellite was upstream of the Earth's bow shock.

The Faraday cup made high-time-resolution measurements of the total charge flux of those positive ions whose velocity component parallel to the satellite-sun line corresponded to an energy per unit charge (E/Q) between 100 and 11,000 volts; this range of E/Q usually included both the protons and alpha particles in the solar wind. The average direction of positive-ion flow could be computed from the relative currents reaching each of four collectors in the Faraday-cup.

At the same time that the ions' total charge flux and direction were measured by the Faraday-cup, a series of voltages was applied to the electrodes of the curved-plate analyzer to obtain the E/Q spectrum of either positive ions or electrons. There were 128 overlapping E/Q channels equally spaced on a logarithmic scale between 2.54 volts and 16.9 kv; alpha particles should appear 10 channels above protons with the same velocity. The instrument usually cycled through a fixed sequence of taking spectra. The majority of spectra in this sequence were 32 channel sweeps about the positive-ion peak; this type of spectrum is called "proton-narrow-fine". It was also possible to sample all 128 channels consecutively ("wide-fine spectra), to sample only every fourth channel ("wide-coarse" spectra), or to reverse the polarity of the voltage and analyze electrons. See Reference 1 and Appendix 2 of Reference 2 for further details.

2. DATA REDUCTION

The computation of plasma parameters was based on the assumption that each ion species in the plasma could be adeuqately described by an isotropic Boltzmann

distribution (density n_i and temperature T_i) in a reference frame moving relative to the detectors with vector velocity $\vec{v}_i$. The method of computing $\vec{v}_i$, n_i, and T_i from the outputs of the Faraday-cup and the curved-plate analyzer is described in detail in Reference 2. Briefly, the process consisted of:

a. Computing the direction of the flux vector from the Faraday-cup data, assuming a cold plasma beam,

b. Using this direction to find the values of v_i, T_i, and n_i for ion species i which best fit the E/Q spectrum measured by the curved-plate analyzer,

c. Correcting the flow direction for the finite temperature T_i of the ions,

d. Using this corrected direction to recompute the values of v_i, T_i, and n_i,

e. Iterating steps c and d until convergence was obtained, and

f. Using the total flux observed by the Faraday-cup, the final direction of the flux vector, and the final velocity value to compute the total charge density n_e of the plasma.

It is known that the distribution of thermal motions in the solar wind is not isotropic. The temperature computed by the method outlined above is thus only a measure of the thermal motions in the solar-antisolar direction; it may be greater than or less than the average temperature, depending on the instantaneous direction of the interplanetary magnetic field.

The angular acceptance cone of the curved-plate analyzer was much narrower than that of the Faraday-cup (5° vs 20° HWHM); thus the curved-plate analyzer cut through only a slice of the distribution function in velocity space while the Faraday-cup accepted almost the entire particle distribution. The total charge density n_e determined in step f of the outline above is considered to be much more reliable than the ion density n_i computed in step d for several reasons:

a. The value of n_i is actually the density of a fictitious isotropic ion distribution with a temperature equal to T_i. If the magnetic field were nearly parallel to or nearly perpendicular to the solar direction, the deviation of the

computed n_i from the true ion density could be large for many combinations of anisotropy, temperature, and flow direction likely to be encountered. The computation of n_e is relatively insensitive to any anisotropy of the plasma; it would enter the calculations only as a correction to the small thermal correction of the flow direction.

b. The value of n_e computed from the Faraday-cup data is much less sensitive to errors or uncertainties in the direction than is the computation of n_i from the curved-plate analyzer data.

c. At large angles of incidence ($>\sim 10^{\circ}$), the values of n_i appear to be consistently too high; this effect is probably related to reflection of glancing incidence particles and other edge effects not studied in sufficient detail during instrument calibration.

The parameter n_i is not completely useless, however; it can be relied upon for the calculation of the alpha/proton density ratio n_α/n_p because the alpha and proton anisotropies were probably aligned with each other.

The accuracy to which the plasma parameters could be determined is discussed in Reference 2.

The OGO data were scanned to determine bow-shock crossing times. All fine-scan positive-ion data upstream of the bow shock were then automatically processed. It was possible, however, for the computer program to reject an ion spectrum for many reasons. The rejection rate over a period of an hour was sometimes zero and sometimes 100%, depending on the properties of the solar wind. Those spectra which survived analysis during periods when the rejection rate was high may have been atypical; an upper limit to the rejection rate over an hour is given by (1 - PCT), where PCT is a parameter given with the hourly averages.

The reasons for rejection of a spectral peak were the following:

a. The spectral scan (after elimination of data immediately following switching of the electrometer from a less sensitive to a more sensitive scale) did not

include data on both sides of the spectral peak.

b. Any current measurement in the spectral peak was a full scale reading (i.e., a 9-bit word = 511) which could be spurious if the electrometer was read out while in the process of changing scales.

c. Any spectral peak which could not be adequately corrected for the anomalous "photodip" in the electrometer zero level. This photodip problem is discussed in more detail in Appendix 2 of Reference 2. The effect severely limited the observation of the solar wind when its velocity was in the range 320 to 400 km/sec.

d. No angular measurement by the Faraday-cup was available.

c. The angle of incidence was greater than 10°.

f. The current at the spectral peak was less than 2×10^{-12} amp for protons or 4×10^{-13} amp for alphas.

g. The thermal Mach number was apparently outside the range of Mach numbers in the comparison table; i.e., $mv^2/2kT$ was either less than 16 or greater than 1000.

h. The variance of the measured data from the curve corresponding to the best-fit parameters v_i, n_i, T_i was anomalously high; in the notation of Reference 2, a spectral peak was rejected if ELSQ > 0.15.

i. The best-fit curve had an unusually strange shape. In the notation of Reference 2, a spectral peak was rejected if |ESKEW| > 0.5 or if |EKURT| > 0.5.

j. The ratio of the proton density n_p to the total charge density n_e was outside the range $0.25 < n_p/n_e < 2$.

k. The computer program did not try to find an alpha-particle peak if the proton peak was rejected for any reason.

l. The alpha-particle peak was also not analyzed if the apparent flow direction changed appreciably (more than a 2° change in either θ_o or ϕ_o, in the notation of Reference 2) between the times at which the proton and alpha peaks were observed.

Only the first reason for rejection was absolutely necessary. It is possible to give special treatment to limited amounts of data to recover some of the rejected spectra. For example, the very low-temperature, high-velocity plasma observed on Feb. 2, 1969 are not included in this collection because of rejection for reason (8); these data have been reprocessed using an expanded comparison table, and can be obtained from M. Neugebauer at JPL (telephone 213-354-5182). Any potential user who is vitally interested in solar wind data for a period of time for which there are little or no data in this collection is invited to discuss the possibility of special processing with M. Neugebauer.

Finally, this collection is limited to positive-ion spectral data in the solar wind. Other types of data which have not yet undergone production processing include:

a. Rapid measurements of total charge flux in the solar wind and magnetosheath. The time resolution of these data usually exceeded the time resolution of the spectral data by a factor of 16.

b. Electron spectra in the magnetosheath and, occasionally, in the magnetosphere.

c. Positive-ion and electron data in the plasmasphere.

3. SPECTRUM-BY-SPECTRUM DATA

A. Magnetic tapes. The tapes were written on a Univac 1108 computer under operating system Exec. 8. They are 7 track tapes written in binary with odd parity. The density is 800 bits per inch. Each tape contains one file and two end-of-file marks.

All data records have the same format, which can be up to 50 words in length. The first seven words in each record are integers, and the rest are floating point, in the standard Univac 1108 representation. The total number of words in each record is 20 plus twice the value of word 19. The words can be interpreted as follows:

Word #	Meaning
1	Day of the year, from 1 to 366
2	Year - 1900
3	Input tape number (of no interest to the general user)
4	Millisec time of day at start of spectrum
5	Spectral type (the only types represented by these data are type 3 which is proton-wide-fine and type 5 which is proton-narrow-fine. The spectral type is of no interest to the general user).
6	Bit rate code (0 or 3 for a data rate of 1 kbps; 1 for 8 kbps; 2 for 64 kbps)
7	Spacecraft clock reading at start of spectrum
8	Total flux, as determined by the Faraday cup measurement made closest to the time of occurrence of the peak current in the curved-plate-analyzer spectrum. Multiply the value of Word 8 by 3×10^6 to get flux in units of charges/cm^2/sec.
9	Cone angle, in degrees. This is the angle between the flux vector and the normal to the Faraday-cup, which is nominally pointed directly toward the sun.
10	Clock angle, in degrees. This is the azimuthal angle between the projection of the flux vector onto the plane of the Faraday-cup and the center of collector number 1. It is measured positively counterclockwise as viewed from the sun. The projection of the flux vector in the solar-ecliptic yz plane is (clock angle - CZ), measured positively from the y_{se} axis toward the z_{se} axis. The parameter CZ is the angle between y_{se} and the center of collector 1; CZ varies slowly in time and is given with the hourly averages.
11	Measurement number at the peak of the proton or alpha spectrum. This parameter can be used to find the time at which the spectral peak was observed by the relation Millisec at peak = (Word 4) + (Word 11) x 2304/kbps, where kbps is 1, 8, or 64 depending on the value of Word 6.
12	Velocity in km/sec.
13	Temperature on 10^3 ^oK.
14	Density n_i in cm^{-3} as determined by the curved-plate analyzer.
15	Density n_e in cm^{-3} as determined by dividing total flux (Word 8) by velocity (Word 12) and a correction for cone angle. This is the total charge density, and it is considered to be more reliable than the density given in Word 14.

Word #	Meaning
16	ELSQ — These parameters give information about how closely the spectral shape resembled that expected for a convected Boltzmann distribution characterized by the parameters given in Words 9, 10, 12, 13 and 14. See Reference 2 for their definition.
17	ESKEW
18	EKURT
19	Number of channels of data used.
20	Particle type: = 1 for protons, 2 for alphas.
21	Channel number.
22	Corrected current in channel given by Word 21.
23	Channel number
24	Corrected current in channel given by Word 23.
Etc.	Etc., pairs of channel numbers and corrected currents.

B. Listing. Some of the parameters given on the tape have also been listed at one line per spectral peak; i.e., if both a proton and an alpha-particle peak were analyzed in any spectrum, that spectrum would have two lines of printout. The listing includes the following information:

Column #	Meaning	Word # on Tape
1	Time at start of spectrum in format HHMMSS, where HH is hours, MM is minutes, and SS is seconds	Calculated from #4
2	Day number	1
3	Year - 1900	2
4	Cone angle	9
5	Clock angle	10
6	Velocity	12
7	Temperature	13
8	Ion density n_i as computed from the curved-plate analyzer data	14
9	Total charge density n_e as determined by combining data from the Faraday-cup with data from the curved-plate analyzer	15

Column #	Meaning	Word # on Tape
10	ELSQ, which is the variance of the data from the best-fit curve.	16
11	ESKEW, which is the excess skew of the measured curve	17
12	EKURT, which is the excess kurtosis of the measured curve	18
13	Type of particle: = 1 for protons, = 2 for alphas	20

See Section 3A for further discussions of the meanings of and units used for the parameters.

A sample listing is included as Figure 3.1.

C. Plots. Graphical displays of the time sequences of some of the computed parameters are also available. Each plot frame contains three hours of data. Sample plots are given in Figures 3.2 and 3.3. The parameters plotted are:

Parameter	Tape Word #	Figure #	Symbol	Range
Proton velocity	12 (20 = 1)	3.2, top	.	200 to 1000 km/sec
Proton temperature	13 (20 = 1)	3.2, bottom	+	10^4 to 10^6 ^oK (log)
Total charge density	15 (20 = 1)	3.2, bottom	.	1 to 100 cm^{-3} (log)
Ecliptic NS angle	Calculated from 9, 10 and CZ (20 = 1)	3.3, top	.	-15 to +15°
Ecliptic EW angle		3.3, top	+	-15 to +15°
Alpha density/ proton density	14 (20 = 2) / 14 (20 = 1)	3.3, bottom	.	0 to 0.5
Alpha temperature/ proton temperature	13 (20 = 2) / 13 (20 = 1)	3.3, bottom	+	0 to 10

The ecliptic angles are defined such that a positive NS angle represents flow from the south towards the north of the ecliptic plane, and a positive EW angle represents flow from the west towards the east of the sun, or some amount of corotation of the plasma with the sun. The EW angle has been corrected for the aberration due to satellite motion.

4. HOURLY-AVERAGE DATA

A. Punched Cards. Hourly averages of many of the plasma parameters are available on punched cards. All spectra on the tape (see Section 3A) were given equal weight in forming the averages. The format of the cards is as follows:

Column #	Fortran Format	Meaning
1 - 3	I3	Year - 1900 (68 to 71)
4 - 7	I4	Day of year (1 to 366)
8 - 10	I3	Hour of day (0 to 23)
11 - 14	I4	Number of proton spectra during the hour
15 - 19	F5.3	PCT = ratio of number of proton spectra during hour to maximum possible number of proton spectra at data rate and width of spectral scan being used. This ratio can be less than 1.0 for many reasons, such as: data gaps, time used for electron spectra or proton-wide-coarse spectra, unacceptable spectra (because angle too large, or couldn't correct for photodip, or poor fit, etc.), and/or time spent in magnetosheath or geomagnetic field.
20 - 24	F5.0	Proton velocity in km/sec
25 - 30	F6.0	Proton temperature in 10^3 ^oK
31 - 36	F6.1	Proton density in cm^{-3}, as determined by the curved-plate analyzer.
37 - 42	F6.1	Total charge density n_e in cm^{-3}, as determined by combining Faraday-cup and curved-plate analyzer data. This is more reliable than the proton density given in columns 31 - 36. See Section 2 for an explanation of the differences.
43 - 48	F6.1	Ecliptic north-south angle in degrees. Positive for flow from south to north of ecliptic.
49 - 54	F6.1	Ecliptic east-west angle in degrees. Positive for flow from west to east of the sun, which means the flow has some amount of corotation with the sun. This angle has been corrected for the effect of the satellite velocity.
55 - 60	F6.0	CZ in degrees = angle between the solar-ecliptic y axis and the center of collector 1.

Column #	Fortran Format	Meaning
61 - 66	F6.3	$(v_\alpha - v_p)/v_p$ = (alpha velocity - proton velocity)/(proton velocity)
67 - 71	F5.1	T_α/T_p = ratio of alpha temperature to proton temperature
72 - 76	F5.3	n_α/n_p = ratio of number density of alphas to number density of protons
77 - 80	I4	Number of alpha-particle spectra during hour.

B. Listing. Figure 4.1 is a sample of the listing of the hourly averages. This listing is a direct printout of the punched cards described above in Section 4A.

C. Plots. The long-term variations of the solar wind have been summarized in 27-day plots of the hourly averages of the proton velocity. Figure 4.2 is a sample of one of these plots.

BIBLIOGRAPHY

A. PAPERS REFERRED TO IN TEXT

(1) GRAHAM, R. A., AND F. E. VESCELUS
OGO E PLASMA SPECTROMETER
PROC. THIRTEENTH NAT. INSTRUM. SOC. AMER. AEROSP. INSTRUM. SYMP., 111-153 (1967).

(2) NEUGEBAUER, M.
COMPUTATION OF SOLAR WIND PARAMETERS FROM THE OGO-5 PLASMA SPECTROMETER DATA USING HERMITE POLYNOMIALS
JPL TECHNICAL MEMORANDUM 33-519 (DEC. 15, 1971).

B. OTHER PAPERS WHOSE MAIN PURPOSE IS THE PRESENTATION OR USE OF OGO-5 PLASMA DATA

NEUGEBAUER, M.
INITIAL DECELERATION OF SOLAR-WIND POSITIVE IONS IN THE EARTH'S BOW SHOCK
JOURNAL OF GEOPHYSICAL RESEARCH 75, 717 (1970).

NEUGEBAUER, M., C. T. RUSSELL, AND J. V. OLSEN
CORRELATED OBSERVATIONS OF ELECTRONS AND MAGNETIC FIELDS AT THE EARTH'S BOW SHOCK
JOURNAL OF GEOPHYSICAL RESEARCH 76, 4366 (1971).

UNTI, T. W. J., G. ATKINSON, C.-S. WU, AND M. NEUGEBAUER
DISSIPATION MECHANISMS IN A PAIR OF SOLAR-WIND DISCONTINUITIES
JOURNAL OF GEOPHYSICAL RESEARCH 77, 2250 (1972).

UNTI, T. W. J., M. NEUGEBAUER, AND B. E. GOLDSTEIN
DIRECT MEASUREMENTS OF SOLAR WIND FLUCTUATIONS BETWEEN 0.0048 AND 13.3 HZ
ASTROPHYSICAL JOURNAL, TO BE PUBLISHED, 1973.

INTRILIGATOR, D. S., AND M. NEUGEBAUER
A SEARCH FOR SOLAR WIND VELOCITY CHANGES BETWEEN 0.75 AU AND 1.0 AU
JOURNAL OF GEOPHYSICAL RESEARCH, SUBMITTED, 1973.

UNTI, T. W. J., M. NEUGEBAUER, AND C. S. WU
THE SHOCK SYSTEM OF FEBRUARY 2, 1969
JOURNAL OF GEOPHYSICAL RESEARCH, SUBMITTED, 1973.

C. OTHER PAPERS IN WHICH OGO-5 PLASMA DATA ARE USED

FREDRICKS, R. W., C. F. KENNEL, F. L. SCARF, G. M. CROOK, AND I. M. GREEN
DETECTION OF ELECTRIC-FIELD TURBULENCE IN THE EARTH'S BOW SHOCK
PHYSICAL REVIEW LETTERS 21, 1761-1764 (1968).

FREDRICKS, R. W., AND P. J. COLEMAN, JR.
OBSERVATIONS OF THE MICROSTRUCTURE OF THE EARTH'S BOW SHOCK
PLASMA INSTABILITIES IN ASTROPHYSICS, D. WENTZEL AND D. TIDMAN, EDITORS,
GORDON AND BREACH PUBLISHERS, NEW YORK (1969).

AUBRY, M. P., C. T. RUSSELL, AND M. G. KIVELSON
ON INWARD MOTION OF THE MAGNETOPAUSE PRECEDING A SUBSTORM
JOURNAL OF GEOPHYSICAL RESEARCH, 75, 7018 (1970).

FREDRICKS, R. W., F. V. CORONITI, C. F. KENNEL, AND F. L. SCARF
FAST TIME RESOLVED SPECTRA OF TURBULENCE IN THE EARTH'S BOW SHOCK
PHYSICAL REVIEW LETTERS, 24, 994-998 (1970).

FREDRICKS, R. W., G. M. CROOK, C. F. KENNEL, I. M. GREEN, F. L. SCARF,
P. J. COLEMAN, JR., AND C. T. RUSSELL
OGO 5 OBSERVATIONS OF ELECTROSTATIC TURBULENCE IN BOW SHOCK MAGNETIC
STRUCTURES
JOURNAL OF GEOPHYSICAL RESEARCH 75, 3751-3768 (1970).

OSTAKOW, S. L., G. W. SHARP, AND K. K. HARRIS
SPECTROMETER OBSERVATIONS IN THE REGION NEAR THE BOW SHOCK ON MARCH 12,
1963
JOURNAL OF GEOPHYSICAL RESEARCH 75, 6024-6036 (1970).

SCARF, F. L., P. J. COLEMAN, JR., R. W. FREDRICKS, C. F. KENNEL, AND
C. T. RUSSELL
MAGNETIC AND ELECTRIC FIELD CHANGES ACROSS THE SHOCK AND IN THE MAGNETO-
SHEATH
INTERCORRELATED SATELLITE OBSERVATIONS RELATED TO SOLAR EVENTS, V. MANNO
AND D. E. PAGE, EDITORS, D. REIDEL PUBLISHING COMPANY, DORDRECHT, HOLLAND
(1970).

SCARF, F. L., R. W. FREDRICKS, L. A. FRANK, C. T. RUSSELL, P. J. COLEMAN, JR.
AND M. NEUGEBAUER
DIRECT CORRELATION OF LARGE AMPLITUDE WAVES WITH SUPRATHERMAL PROTONS IN
THE UPSTREAM SOLAR WIND
JOURNAL OF GEOPHYSICAL RESEARCH 75, 7316 (1970).

SCARF, F. L., R. W. FREDRICKS, I. M. GREEN AND M. NEUGEBAUER
OGO-5 OBSERVATIONS OF QUASI-TRAPPED ELECTROMAGNETIC WAVES IN THE SOLAR
WIND
JOURNAL OF GEOPHYSICAL RESEARCH 75, 3735 (1970).

AUBRY, M. P., M. G. KIVELSON, AND C. T. RUSSELL
MOTION AND STRUCTURE OF THE MAGNETOPAUSE
JOURNAL OF GEOPHYSICAL RESEARCH, 76, 1673 (1971).

RUSSELL, C. T., C. R. CHAPPELL, M. D. MONTGOMERY, M. NEUGEBAUER, AND F. L. SCARF
OGO 5 OBSERVATIONS OF THE POLAR CUSP ON NOVEMBER 1, 1968
JOURNAL OF GOEPHYSICAL RESEARCH 76, 6743 (1971).

RUSSELL, C. T., D. D. CHILDERS, AND P. J. COLEMAN, JR.
OGO-5 OBSERVATIONS OF UPSTREAM WAVES IN THE INTERPLANETARY MEDIUM. DISCRETE WAVE PACKETS
JOURNAL OF GEOPHYSICAL RESEARCH, 76, 845 (1971).

SCARF, F. L., R. W. FREDRICKS, L. A. FRANK, AND M. NEUGEBAUER
NONTHERMAL ELECTRONS AND HIGH-FREQUENCY WAVES IN THE UPSTREAM SOLAR WIND
JOURNAL OF GEOPHYSICAL RESEARCH 76, 5162 (1971).

FREDRICKS, R. W., F. L. SCARF, C. T. RUSSELL, AND M. NEUGEBAUER
DETECTION OF SOLAR-WIND ELECTRON PLASMA FREQUENCY FLUCTUATIONS IN AN OBLIQUE NONLINEAR MAGNETOHYDRODYNAMIC WAVE
JOURNAL OF GEOPHYSICAL RESEARCH 77, 3598 (1972).

GUHA, J. K., D. L. JUDGE, AND J. H. MARBURGER
OGO-5 MAGNETIC FIELD MEASUREMENTS NEAR THE EARTH'S BOW SHOCK. A CORRELATION WITH THEORY
JOURNAL OF GEOPHYSICAL RESEARCH, 77, 604-610 (1972).

NEUGEBAUER, M., C. W. SNYDER, D. R. CLAY, AND B. E. GOLDSTEIN
SOLAR WIND OBSERVATIONS ON THE LUNAR SURFACE WITH APOLLO 12 ALSEP
PLANETARY AND SPACE SCIENCE 20, 1703 (1972).

SCARF, F. L., R. W. FREDRICKS, I. M. GREEN, AND C. T. RUSSELL
PLASMA WAVES IN THE DAYSIDE POLAR CUSP 1. MAGNETOSPHERIC OBSERVATIONS
JOURNAL OF GEOPHYSICAL RESEARCH 77, 2274-2293 (1972).

SCARF, F. L., R. W. FREDRICKS, E. J. SMITH, A. M. A. FRANDSEN, AND G. P. SERBU
OGO 5 OBSERVATIONS OF LHR NOISE, EMISSIONS, AND WHISTLERS NEAR THE PLASMAPAUSE AT SEVERAL EARTH RADII DURING A LARGE MAGNETIC STORM
JOURNAL OF GEOPHYSICAL RESEARCH 77, 1776-1793 (1972).

OSSAKOW, S. L., AND G. W. SHARP
PROTON SCATTERING IN THE REGION NEAR THE EARTH'S BOW SHOCK
JOURNAL OF GEOPHYSICAL RESEARCH 78, 607-616 (1973).

BURLAGA, L. F., J. RAHE, B. DONN, AND M. NEUGEBAUER
SOLAR WIND INTERACTION WITH COMET BENNETT (1969I)
SOLAR PHYSICS, TO BE PUBLISHED, 1973.

FREDRICKS, R. W., AND C. T. RUSSELL
ION CYCLOTRON WAVES OBSERVED IN THE POLAR CUSP
JOURNAL OF GEOPHYSICAL RESEARCH, ACCEPTED FOR PUBLICATION (1973).

FREDRICKS, R. W., F. L. SCARF, AND C. T. RUSSELL
FIELD-ALIGNED CURRENTS, PLASMA WAVES AND ANOMALOUS RESISTIVITY IN THE DISTURBED POLAR CUSP
JOURNAL OF GEOPHYSICAL RESEARCH, ACCEPTED FOR PUBLICATION (1973).

SCARF, F. L., R. W. FREDRICKS, C. T. RUSSELL, M. KIVELSON, M. NEUGEBAUER, AND C. R. CHAPPELL
OBSERVATION OF A CURRENT-DRIVEN PLASMA INSTABILITY AT THE OUTER ZONE - PLASMA SHEET BOUNDARY
JOURNAL OF GEOPHYSICAL RESEARCH, TO BE PUBLISHED, 1973.

KAELSON, M. G., C. T. RUSSELL, M. NEUGEBAUER, F. L. SCARF, AND R. W. FREDRICKS
THE DEPENDENCE OF THE POLAR CUSP ON THE NORTH-SOUTH COMPONENT OF THE INTERPLANETARY MAGNETIC FIELD
JOURNAL OF GEOPHYSICAL RESEARCH, TO BE PUBLISHED, 1973.

Figure 3.1

1046	81	68	1.74	-36.00	566.28	98.39	1.75	2.16	.0413	-.1833	.0765
1046	81	68	2.34	-31.43	570.12	505.14	.07	2.18	.0435	.0201	.1839
1105	81	68	3.57	-29.75	576.77	114.08	2.25	2.13	.0053	-.0148	-.0043
1105	81	68	3.36	-35.68	570.77	512.71	.08	2.21	.0450	-.0035	.1920
1115	81	68	3.53	-23.47	568.57	116.47	2.29	2.11	.0014	-.0272	-.0395
1115	81	68	3.05	-37.76	564.70	417.91	.07	2.21	.0077	-.0365	-.0119
1212	81	68	1.79	-60.18	565.76	93.21	1.84	2.55	.0216	-.1566	.0539
1212	81	68	3.26	-50.98	573.71	553.60	.10	2.77	.0240	.0396	.1314
1240	81	68	3.39	-64.58	560.05	95.84	2.16	2.58	.0106	-.1205	-.0765
1240	81	68	2.78	-71.00	571.04	472.31	.09	2.47	.0245	.0112	.1959
1250	81	68	4.44	-68.44	561.79	73.84	2.10	2.43	.0023	-.0528	-.0054
1250	81	68	2.91	-71.57	570.28	512.39	.10	2.48	.0365	-.0134	.2620
1309	81	68	2.62	-101.91	562.08	60.47	1.27	2.51	.0079	-.0894	.1300
1318	81	68	3.21	-140.92	557.67	83.16	1.87	2.46	.0110	-.1159	-.0242
1318	81	68	.99	-81.59	570.90	451.88	.09	2.37	.0472	.0001	.2119
1328	81	68	.93	-114.28	562.68	92.05	1.78	2.60	.0149	-.0234	.0658
1328	81	68	1.92	-85.99	564.17	756.10	.13	2.58	.0405	.1242	.0570
1347	81	68	1.76	-80.26	563.45	88.09	1.89	2.33	.0093	-.1345	-.0609
1347	81	68	1.47	-77.84	574.16	399.13	.08	2.46	.0483	-.0073	.3134
1356	81	68	3.02	-50.32	566.80	90.84	2.06	2.42	.0181	-.1596	.0236
1356	81	68	2.96	45.09	570.32	414.33	.09	2.41	.0454	.0253	.2609
1425	81	68	4.74	-95.33	590.47	109.68	2.25	2.29	.0019	-.0361	.0143
1425	81	68	3.68	-109.58	573.27	630.25	.13	2.41	.0122	.0384	-.0033
1434	81	68	4.87	-111.01	582.42	96.27	2.42	2.49	.0039	-.0140	.0047
1434	81	68	4.46	-107.11	576.65	382.65	.11	2.27	.0402	-.0221	.2557
1453	81	68	3.33	-93.93	584.11	85.30	1.69	2.46	.0433	-.0693	.1316
1453	81	68	2.45	-73.95	576.35	608.15	.12	2.40	.0175	.0018	.0274
1503	81	68	3.97	-56.45	592.40	146.18	2.72	2.38	.0095	.0609	-.0561
1503	81	68	2.36	-31.43	576.39	620.23	.12	2.51	.0178	.0791	.1432
1512	81	68	3.12	-35.11	590.86	123.68	2.41	2.34	.0063	.0337	-.0217
1522	81	68	3.22	-87.84	584.23	90.34	1.71	2.40	.0045	-.0715	.1262
1522	81	68	1.78	-47.23	575.68	580.57	.11	2.49	.0121	.0086	.0036
1822	81	68	3.29	-93.79	587.91	119.54	2.05	2.36	.0087	-.0063	.0231
2104	81	68	2.36	-62.33	589.82	111.36	2.11	2.42	.0056	.0455	-.0341
2104	81	68	2.77	-63.52	570.87	567.02	.10	2.43	.0435	.0774	.0920
2113	81	68	2.07	-79.88	580.42	71.48	1.42	2.30	.1411	-.0990	.2239
2336	81	68	1.10	-4.93	589.81	83.52	1.94	2.31	.0076	.0144	.0297
2336	81	68	1.45	-22.06	572.61	516.92	.10	2.43	.0092	.0631	.0230
2346	81	68	1.40	-46.04	590.23	102.51	2.00	2.33	.0082	.0620	-.0266
2346	81	68	1.24	-26.31	571.84	562.82	.10	2.33	.0121	.0696	.0272
2414	81	68	1.19	-4.54	589.65	108.95	2.24	2.28	.0050	.0214	-.0270
2414	81	68	.98	-10.83	575.01	491.43	.10	2.41	.0151	.0446	.0489
2424	81	68	1.52	24.07	584.46	121.16	2.24	2.37	.0065	.0935	-.0850
2424	81	68	.57	-9.67	571.15	530.99	.11	2.44	.0174	.0622	.0643
2606	81	68	.67	-97.41	588.83	130.79	2.29	2.30	.0084	.0070	-.0771
2616	81	68	2.09	-56.94	591.26	82.4[illegible]	2.04	1.90	.0379	-.0381	-.056[illegible]
2616	81	68	1.73	-44.30	571.80	322.[illegible]	.06	1.86	.0243	[illegible]	[illegible]

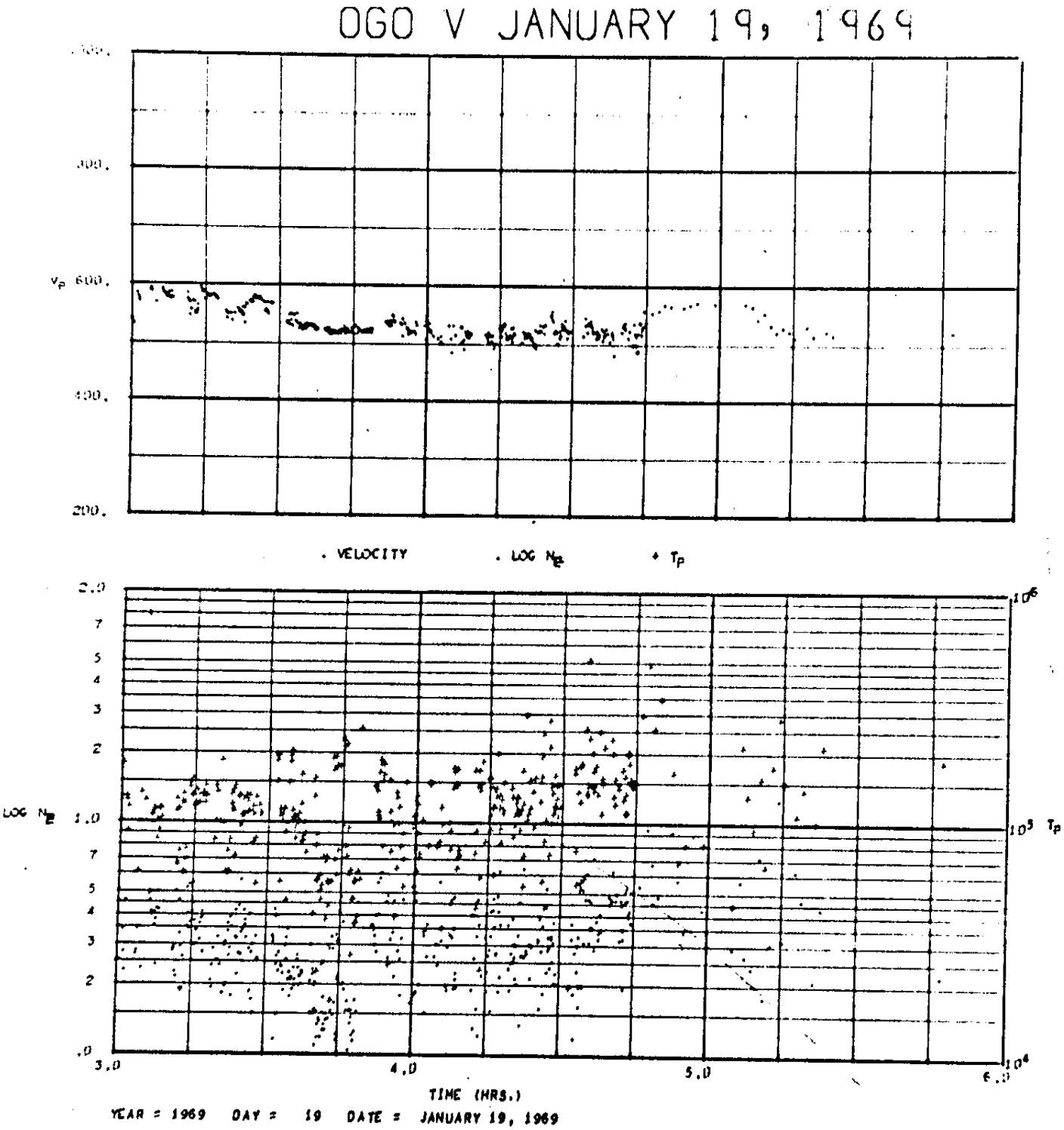
OGO V JANUARY 19, 1969
V_P 600.
400.
200.
. VELOCITY
. LOG N_E
+ T_P
LOG N_E
2.0
1.0
.0
10^6
10^5
10^4
T_P
3.0
4.0
5.0
6.0
TIME (HRS.)
YEAR = 1969 DAY = 19 DATE = JANUARY 19, 1969

Figure 3.2

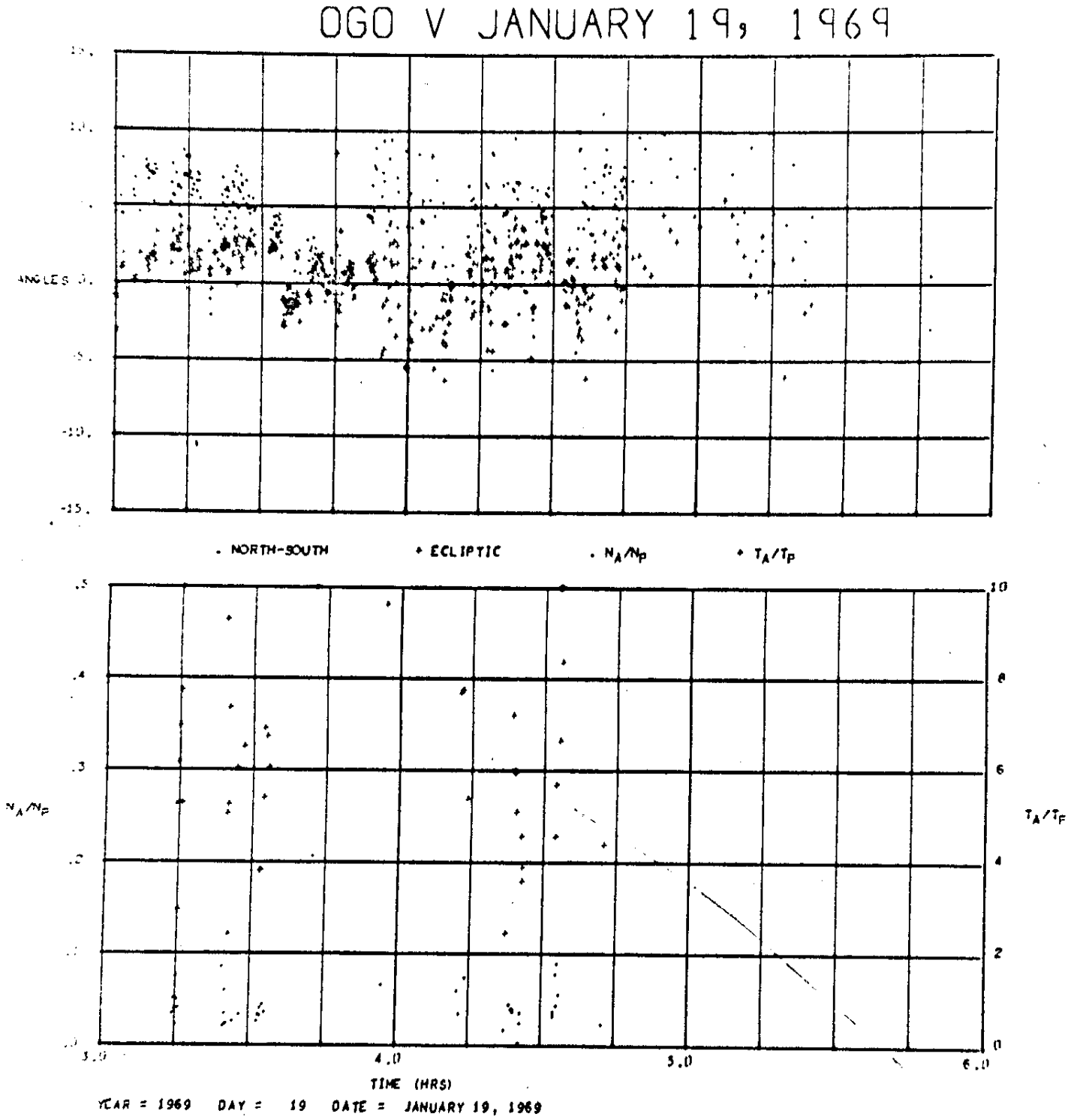
OGO V JANUARY 19, 1969
ANGLES
-10.
-15.
NORTH-SOUTH
ECLIPTIC
N_A/N_P
T_A/T_P
.5
.4
.3
.2
10
8
6
4
2
0
3.0
4.0
5.0
6.0
TIME (HRS)
YEAR = 1969 DAY = 19 DATE = JANUARY 19, 1969

Figure 3.3

Figure 7.1

68	102	19	41	.872	374.	34.	38.9	47.8	1.4	3.1	-6.	-.004	2.8	.046	27
	102	20	31	.660	374.	29.	21.3	23.6	2.1	3.3	-6.	-.009	3.0	.024	26
68	102	21	19	.404	367.	31.	20.4	22.0	2.3	4.6	-6.	-.007	2.5	.023	14
68	103	4	4	.011	385.	81.	11.0	10.5	6.2	-1.2	-13.	-.053	7.6	.067	2
68	103	5	1	.006	373.	81.	15.5	16.9	2.9	-2.1	-14.	.000	.0	.000	0
68	103	6	3	.052	395.	39.	19.8	19.1	.9	.1	-15.	-.013	4.9	.022	1
68	104	1	6	.033	469.	278.	7.9	20.2	6.9	4.7	5.	.000	.0	.000	0
68	104	2	107	.282	452.	191.	8.2	13.1	.5	-2.6	5.	.083	6.5	.067	6
68	104	3	67	.362	447.	130.	6.3	10.1	-.1	-3.0	4.	.084	9.4	.099	2
68	104	4	11	.234	467.	112.	6.3	9.7	-2.0	-2.2	4.	.000	.0	.000	0
68	104	5	162	.547	481.	171.	7.4	10.6	-1.8	-.8	3.	.042	7.3	.053	95
68	104	6	239	.631	475.	146.	6.9	9.1	-1.9	-.3	3.	.039	6.7	.049	179
68	104	7	45	.600	491.	144.	6.5	7.5	-3.5	1.2	3.	.015	5.3	.050	40
68	104	8	25	.532	474.	131.	6.4	6.5	1.5	1.3	2.	.056	8.0	.046	11
68	104	9	39	.830	534.	117.	5.5	5.9	-1.3	1.5	2.	-.019	4.1	.024	24
68	104	10	25	.532	503.	106.	4.7	5.3	-.9	.5	2.	.065	5.1	.030	6
68	104	11	216	.570	502.	99.	4.3	6.1	-.5	2.4	0.	.053	10.9	.070	116
68	104	12	187	.577	507.	135.	5.2	6.6	-.6	3.1	0.	.029	8.0	.064	139
68	104	13	28	.596	559.	130.	5.5	5.9	-2.6	1.6	-1.	-.039	4.6	.035	26
68	104	14	24	.511	474.	160.	5.8	5.5	-.1	3.5	-2.	.020	5.0	.055	5
68	104	15	71	.449	487.	126.	4.6	4.9	-.4	3.2	-2.	.047	7.9	.075	28
68	104	16	147	.388	487.	119.	4.2	4.6	.7	3.2	-2.	.046	8.3	.078	54
68	104	17	224	.591	520.	155.	5.1	6.3	-1.3	.5	-2.	.042	7.1	.076	191
68	104	18	198	.522	526.	130.	4.9	6.2	-.7	.6	-3.	.043	7.9	.067	155
68	104	19	73	.193	521.	115.	4.6	5.9	.4	1.0	-3.	.056	9.6	.072	65
68	104	23	27	.574	525.	157.	4.9	4.4	1.4	-1.0	-4.	.063	4.2	.045	6
68	105	0	13	.277	524.	124.	4.2	3.8	.2	1.6	-4.	.074	4.8	.036	2
68	105	10	6	.128	569.	160.	3.6	3.3	1.3	-2.5	-9.	.047	3.3	.069	3
68	105	11	17	.362	579.	135.	3.6	3.1	3.3	-2.7	-9.	.041	3.9	.067	5
68	105	13	10	.213	530.	110.	3.9	3.0	-.9	4.4	-10.	.000	.0	.000	0
68	105	14	30	.190	540.	164.	4.3	3.2	-6.1	-1.4	-10.	.062	5.6	.091	12
68	105	15	154	.406	553.	101.	3.2	3.2	2.2	-1.0	-11.	.057	11.0	.099	95
68	105	16	70	.185	509.	66.	3.4	3.8	-.2	2.9	-12.	.058	16.3	.078	18
68	105	17	80	.211	528.	78.	3.8	3.6	1.7	3.5	-13.	.038	11.7	.071	32
68	107	1	32	.084	606.	119.	2.2	2.4	1.5	1.5	0.	.084	6.7	.052	6
68	107	2	10	.026	610.	152.	2.4	2.2	2.5	2.4	-1.	.026	8.0	.067	2
68	107	3	18	.047	605.	172.	2.1	2.2	1.1	2.8	-1.	.066	8.0	.113	5
68	107	4	21	.055	617.	221.	2.6	2.2	1.0	2.1	-1.	-.009	9.7	.108	6
68	107	5	12	.032	632.	133.	2.2	1.7	2.4	2.4	-2.	.000	.0	.000	0
68	107	7	10	.213	617.	310.	2.8	2.4	.9	-1.3	-2.	.139	1.7	.023	1
68	107	8	8	.170	603.	163.	1.5	1.8	.0	1.9	-3.	.097	6.3	.061	1
68	107	10	14	.298	642.	225.	1.6	1.4	-.4	2.3	-4.	.008	2.3	.034	5
68	107	12	43	.162	595.	249.	2.4	1.6	1.1	4.2	-5.	.055	6.5	.077	29
68	107	13	113	.298	592.	222.	2.5	1.8	-.4	4.2	-4.	.058	6.8	.067	48
68	107	14	69	.182	577.	160.	2.3	1.7	1.3	4.6	-5.	.026	5.9	.055	21
68	107	15	136	.359	526.	118.	2.4	2.1	.2	4.7	-6.	.057	10.7	.094	22
68	107	16	3	.064	509.	194.	3.8	2.5	-6.0	2.5	-5.	.000	.0	.000	0
68	107	17	10	.213	498.	164.	3.0	2.6	-4.8	2.9	-6.	.000	.0	.000	0
68	107	18	19	.196	517.	168.	3.4	3.2	-3.7	4.3	-6.	.044	5.9	.057	1
68	107	19	141	.372	558.	190.	2.8	2.7	-1.6	1.9	-7.	.000	6.3	.074	99
68	107	20	144	.537	533.	172.	2.6	2.6	-1.0	.6	-7.	.023	6.0	.092	35
68	107	21	17	.362	521.	167.	3.6	3.1	-.9	4.1	-8.	.000	.0	.000	0
	107	22	7	.149	547.	152.	3.2	3.0	-3.3	-.8	-8.	.073	1.7	.026	2
68	107	23	35	.745	535.	182.	3.7	3.4	-4.0	1.0	-8.	.048	2.6	.023	5
68	108	0	19	.404	514.	146.	3.5	3.5	-.6	2.8	-9.	.000	.0	.000	0
68	108	1	9	.191	516.	89.	2.2	2.8	1.4	4.7	-10.	.089	8.6	.069	2
68	108	2	13	.277	506.	118.	2.5	2.2	1.9	4.3	-10.	.000	.0	.000	0

Figure 4.2

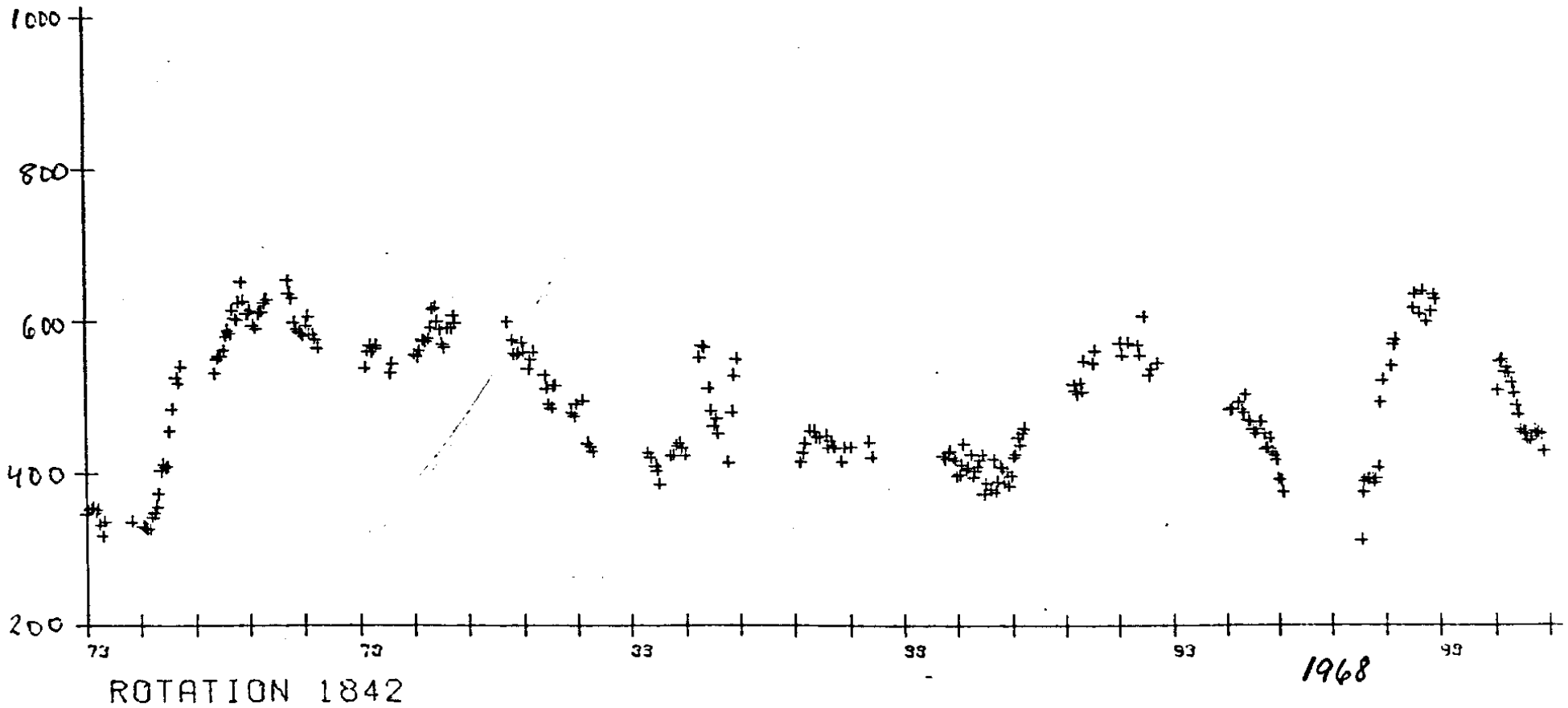

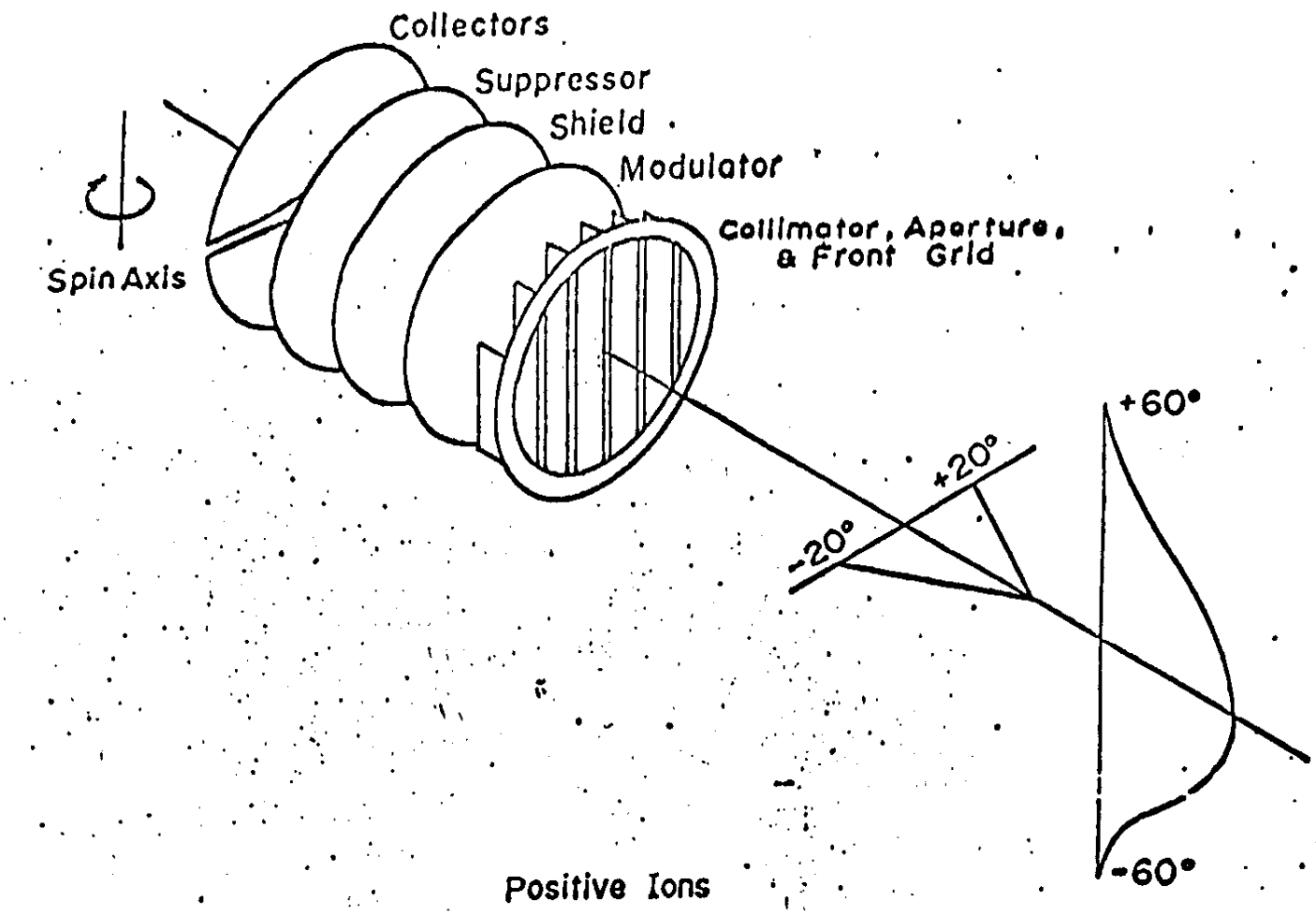

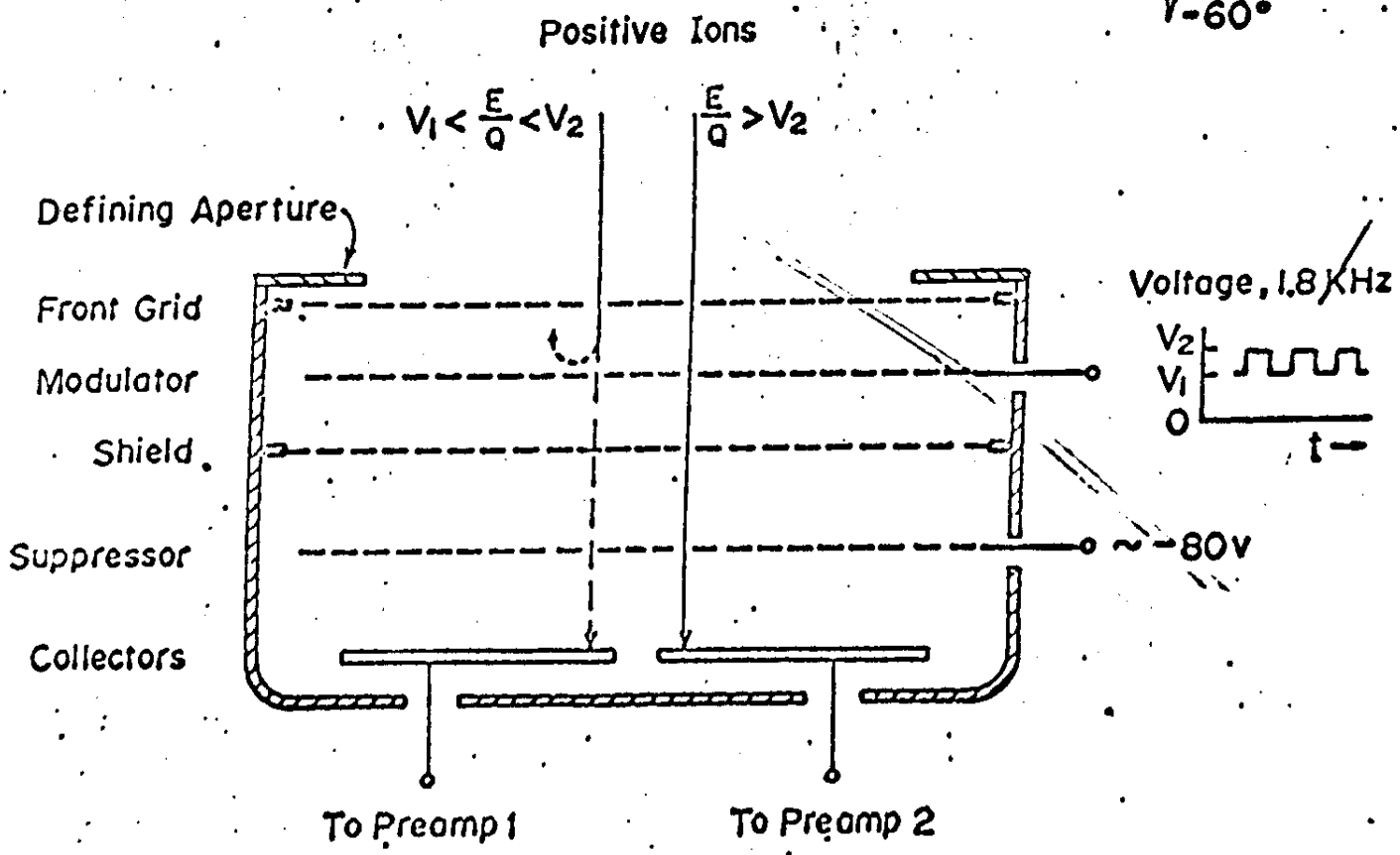

Figure 4-1

After p 4-1

	Sector 1	2	3	4	5	6	7	8	9	10	11	12	13		
Ions - Level 1	F	F													
Ions - Level 2	S													F	M
Ions - Level 3	S													H	M
Ions - Level 4	S													H	M
Ions - Level 5	S													H	M
Ions - Level 6	S													H	M
Ions - Level 7	S													H	M
Electrons - Level 1, 2, 3 or 4	S													H	M
Calibration	S													H	M
Ions - Level 8	C													F	C
Ions - Level 9	S													H	M
Ions - Level 10	S													H	M
Ions - Level 11	S													H	M
Ions - Level 12	S													H	M
Ions - Level 13	S													H	M
Ions - Level 14	S													H	M
														H	M

F = Fixed word

H = High voltage calibrate

M = Maximum half-collector current

S = Sector having maximum half-collector current (from previous energy level)

C = Additional calibration words.

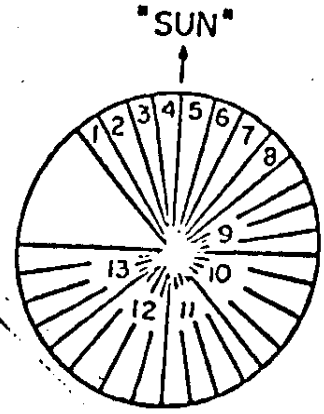

Figure 4 - 2 The data taking sequence. Each row corresponds to a different energy interval and is filled during one spacecraft rotation. The current is averaged over 11.25° angular intervals as the spacecraft spins. For the 45° sectors, 9-13, only the maximum of the four 11.25° subsector average currents is recorded.

After p 4-2

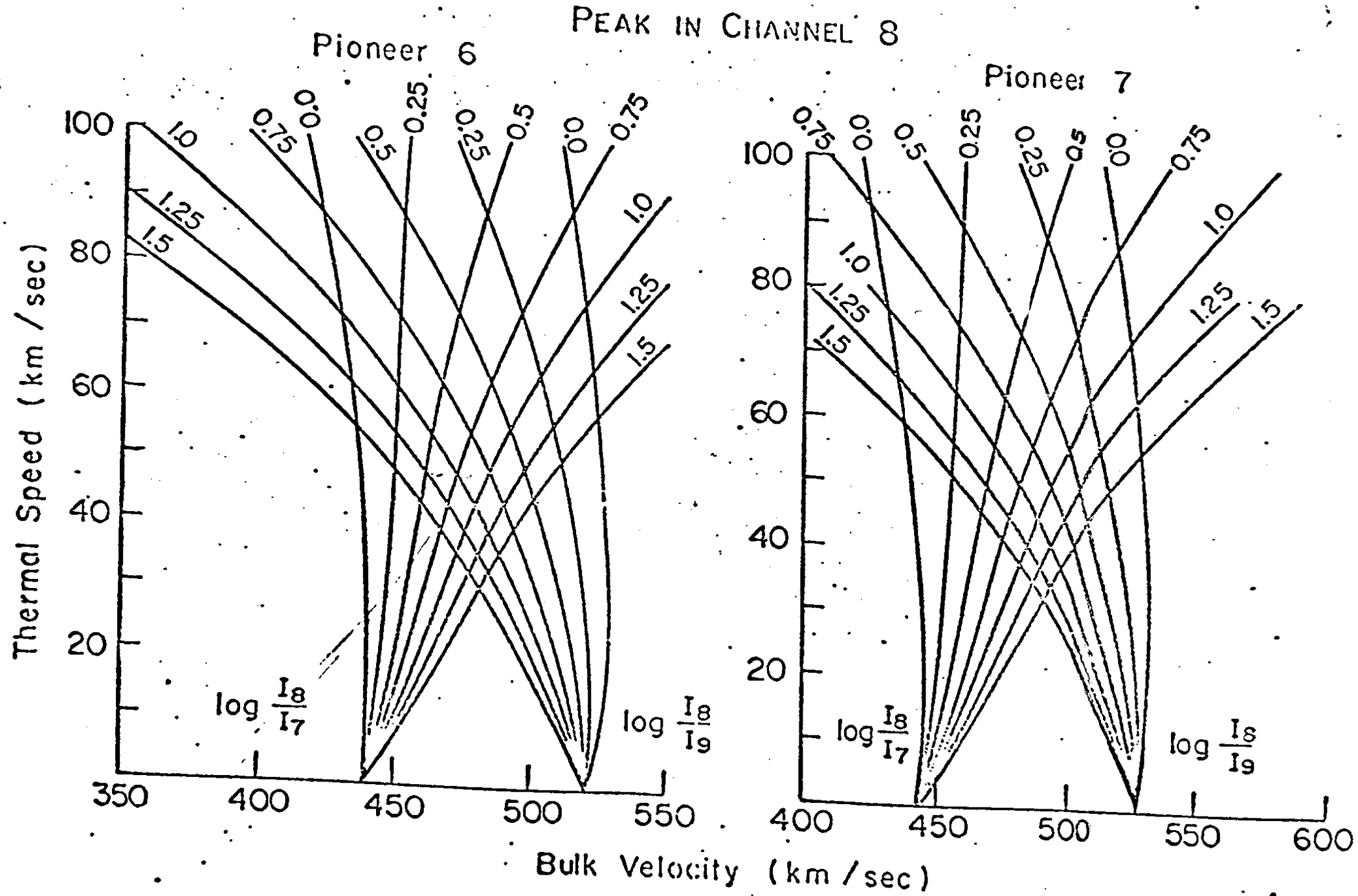

Figure 4-3

After p 4-7

REC #

1	68	65	23	131	.346	382.	52.	2.8	5.1	-.8	-2.9	11.	.000	.0	.000	0
2	68	66	0	95	.251	386.	74.	3.3	4.6	2.8	-.7	12.	-.059	.3	.024	1
3	68	66	1	247	.652	399.	83.	3.8	4.3	2.5	-.2	12.	.000	.0	.000	0
4	68	66	2	263	.694	401.	92.	3.9	3.8	3.1	-.6	12.	.000	.0	.000	0
5	68	66	3	272	.718	398.	95.	4.0	3.8	.7	.3	11.	.000	.0	.000	0
6	68	66	4	229	.604	390.	115.	3.6	3.8	.8	-.1	12.	.000	.0	.000	0
7	68	66	5	249	.657	397.	103.	2.8	3.1	-.1	1.2	12.	.000	.0	.000	0
8	68	66	6	276	.728	403.	93.	3.3	3.4	1.3	1.7	12.	.000	.0	.000	0
9	68	66	7	261	.689	402.	76.	3.2	3.6	-.5	1.4	12.	.000	.0	.000	0
10	68	66	8	233	.615	411.	67.	3.3	3.5	2.2	2.3	12.	.000	.0	.000	0
11	68	66	9	57	.150	420.	68.	3.3	3.3	3.3	3.1	12.	.000	.0	.000	0
12	68	66	10	4	.085	409.	96.	4.3	3.5	-1.4	4.0	12.	.000	.0	.000	0
13	68	66	11	223	.544	409.	81.	3.5	3.6	.7	3.0	11.	.000	.0	.000	0
14	68	66	12	246	.649	391.	73.	3.3	3.4	1.2	2.0	12.	.000	.0	.000	0
15	68	66	13	238	.628	415.	68.	3.1	2.8	3.1	4.4	12.	.000	.0	.000	0
16	68	66	14	239	.631	427.	52.	2.7	2.6	3.6	3.5	12.	.000	.0	.000	0
17	68	66	15	260	.686	423.	71.	3.2	3.0	3.2	3.6	12.	.000	.0	.000	0
18	68	66	16	297	.567	444.	75.	3.3	3.1	3.9	.6	12.	.000	.0	.000	0
19	68	66	17	11	.029	430.	63.	2.9	2.7	2.9	2.3	14.	.000	.0	.000	0
20	68	66	18	21	.046	404.	89.	2.7	2.9	1.4	2.8	13.	.000	.0	.000	0
21	68	67	19	20	.031	375.	53.	4.2	3.5	4.4	1.9	9.	.000	.0	.000	0
22	68	67	20	73	.193	371.	50.	3.1	3.6	4.4	2.6	10.	.000	.0	.000	0
23	68	67	21	57	.150	373.	36.	3.3	3.7	.6	4.5	10.	.000	.0	.000	0
24	68	67	22	88	.232	392.	35.	2.9	3.7	2.8	3.5	10.	.000	.0	.000	0
25	68	67	23	37	.098	348.	39.	3.2	4.0	3.7	3.8	10.	.000	.0	.000	0
26	68	68	0	18	.047	343.	37.	3.3	4.5	1.9	2.7	10.	.000	.0	.000	0
27	68	68	1	76	.201	371.	30.	3.3	4.6	3.6	3.0	10.	.000	.0	.000	0
28	68	68	2	15	.040	360.	40.	3.4	3.9	2.6	4.3	10.	.000	.0	.000	0
29	68	68	3	70	.185	360.	47.	3.4	4.2	1.3	2.8	9.	.000	.0	.000	0
30	68	68	4	40	.106	359.	50.	3.2	4.3	1.5	2.4	9.	.000	.0	.000	0
31	68	68	5	38	.100	359.	34.	2.8	4.2	1.8	2.6	10.	.011	1.8	.016	1
32	68	68	6	35	.092	370.	29.	2.9	3.8	1.6	2.8	10.	-.012	3.7	.021	7
33	68	68	7	16	.042	352.	32.	3.3	3.6	1.3	2.9	9.	-.010	5.6	.029	1
34	68	68	8	8	.013	353.	39.	3.5	3.4	2.5	3.4	10.	.000	.0	.000	0
35	68	68	9	20	.029	366.	35.	3.2	3.3	2.7	2.7	10.	-.066	6.3	.048	6
36	68	68	10	208	.300	385.	45.	2.6	3.1	3.0	2.1	10.	.000	.0	.000	0
37	68	68	11	146	.210	361.	44.	2.6	2.8	1.5	3.1	9.	.000	.0	.000	0
38	68	68	12	3	.005	349.	26.	3.1	3.3	3.0	3.8	10.	.000	.0	.000	0
39	68	68	13	2	.005	334.	29.	3.6	3.2	1.8	4.7	11.	.000	.0	.000	0
40	68	68	14	1	.003	326.	19.	3.6	3.6	2.9	4.0	10.	.000	.0	.000	0
41	68	68	15	1	.002	329.	40.	3.2	3.9	2.6	4.4	10.	.000	.0	.000	0
42	68	68	16	9	.013	341.	20.	2.8	3.6	3.9	4.1	10.	-.022	9.0	.047	2
43	68	68	17	8	.012	336.	28.	3.1	4.3	2.5	4.3	10.	.017	6.4	.033	2
44	68	68	21	11	.029	347.	14.	2.4	5.2	3.6	1.2	9.	.000	.0	.000	0
45	68	68	22	2	.005	294.	8.	1.6	4.6	1.5	3.6	10.	.000	.0	.000	0
46	68	68	23	5	.013	289.	12.	2.8	6.5	1.2	1.4	9.	.000	.0	.000	0
47	68	69	0	9	.024	291.	9.	2.9	5.8	.5	1.7	10.	.058	2.7	.029	1
48	68	69	1	1	.003	318.	18.	5.3	6.1	2.9	4.5	10.	-.001	1.4	.017	1
49	68	69	3	3	.008	292.	6.	3.1	5.8	.4	3.3	9.	.000	.0	.000	0
50	68	69	4	1	.003	285.	11.	2.9	7.0	1.2	2.0	9.	.000	.0	.000	0
51	68	69	5	1	.003	313.	7.	3.0	5.4	4.1	3.9	10.	.000	.0	.000	0
52	68	70	6	1	.003	313.	48.	11.2	17.9	3.4	2.0	9.	-.018	2.1	.017	1
53	68	70	7	10	.020	333.	36.	12.4	16.7	2.9	2.9	9.	.007	5.6	.030	7
54	68	70	8	5	.010	331.	25.	10.8	15.7	2.0	5.8	10.	.015	3.6	.025	4
55	68	70	12	73	.193	349.	36.	19.2	24.7	.9	5.1	9.	-.002	2.3	.022	73
56	68	70	13	170	.449	358.	40.	19.0	24.0	1.1	4.3	9.	-.001	2.4	.024	168
57	68	70	14	49	.129	363.	45.	15.3	20.1	1.7	4.1	9.	-.005	4.7	.032	49
58	68	70	15	61	.161	359.	57.	10.5	16.0	.2	3.2	9.	-.006	5.1	.047	59

TIME SPAN
3/05/68 - 4/30/71

MODCOMP ASCII

DATAFOLD FORMS, INC - W

59	68	70	16	47	.124	366.	105.	5.1	8.8	-1.2	.5	9.	-.025	9.5	.117	5
60	68	70	17	141	.372	367.	132.	5.5	7.5	-2.4	-.1	9.	.000	.0	.000	0
61	68	70	18	180	.475	377.	113.	5.8	9.3	-3.2	-.8	9.	-.061	8.3	.091	11
62	68	70	19	157	.414	387.	136.	5.6	9.0	-2.1	-1.2	8.	-.072	8.7	.129	2
63	68	70	20	206	.544	386.	184.	4.7	9.1	-1.7	-1.8	8.	.000	.0	.000	0
64	68	70	21	197	.520	383.	143.	5.3	8.9	-.9	-1.7	8.	.000	.0	.000	0
65	68	70	22	174	.459	378.	128.	6.4	8.9	-1.7	-1.0	9.	.000	.0	.000	0
66	68	70	23	134	.354	371.	107.	5.4	8.3	-2.2	-.1	9.	.000	.0	.000	0
67	68	71	0	10	.026	362.	52.	5.6	9.3	-1.3	2.5	8.	.004	5.1	.051	9
68	68	71	1	15	.040	361.	46.	8.1	10.9	-.1	3.2	8.	.007	4.2	.043	14
69	68	71	2	14	.037	368.	53.	9.2	13.9	.9	2.0	8.	-.003	3.7	.056	13
70	68	71	3	14	.037	378.	63.	9.6	14.5	.3	1.2	8.	-.014	4.3	.072	14
71	68	71	4	25	.066	372.	59.	8.8	14.1	2.7	1.5	7.	-.008	3.9	.091	24
72	68	71	5	19	.050	377.	55.	7.2	12.3	2.1	-.2	8.	-.008	4.0	.093	19
73	68	71	6	47	.124	381.	80.	8.8	12.8	2.1	-.7	8.	-.001	4.3	.080	47
74	68	71	7	42	.111	384.	104.	9.8	12.4	1.9	-1.7	8.	.012	4.5	.072	36
75	68	71	8	67	.127	384.	113.	10.7	12.6	1.4	-1.4	8.	.026	4.7	.066	44
76	68	71	9	56	.081	377.	68.	7.6	12.2	1.3	-1.0	7.	.050	5.2	.071	41
77	68	71	10	75	.108	390.	55.	5.2	9.3	.2	-1.0	8.	.026	5.1	.085	75
78	68	71	11	10	.022	383.	57.	7.5	10.0	1.9	-.3	8.	.012	4.1	.046	10
79	68	71	12	51	.135	379.	58.	6.8	9.0	1.0	-1.2	7.	.002	3.6	.047	50
80	68	71	13	25	.066	371.	103.	7.5	9.3	.9	-1.0	8.	.012	3.3	.049	12
81	68	71	14	112	.296	376.	126.	7.5	9.9	1.2	-1.2	8.	-.004	4.2	.085	39
82	68	71	15	35	.064	388.	54.	5.7	7.7	2.1	-.8	7.	.022	5.4	.053	35
83	68	71	16	41	.059	388.	57.	7.0	8.7	2.3	-1.2	8.	.019	4.6	.046	41
84	68	71	17	10	.014	381.	52.	5.8	9.0	2.0	.0	7.	.039	3.7	.045	8
85	68	71	18	22	.032	376.	56.	6.5	9.5	2.3	-.5	8.	.031	3.8	.050	13
86	68	71	19	31	.045	382.	97.	8.4	7.8	4.5	2.0	6.	.017	4.0	.070	26
87	68	71	20	42	.062	378.	78.	7.8	8.6	2.0	.7	7.	.005	3.7	.069	34
88	68	71	21	34	.090	379.	74.	8.1	9.8	3.2	-.2	7.	.004	3.2	.063	22
89	68	71	22	30	.079	387.	62.	6.5	8.6	1.0	-.4	7.	.003	3.4	.063	30
90	68	71	23	57	.150	388.	111.	7.5	8.2	1.7	-1.4	7.	.004	3.4	.043	25
91	68	72	20	1	.003	344.	45.	6.7	12.7	2.2	2.4	9.	.004	2.6	.057	1
92	68	72	21	52	.137	347.	55.	6.4	12.7	.5	.1	8.	-.010	4.4	.084	41
93	68	72	22	31	.082	349.	46.	5.6	11.6	-.8	1.7	8.	-.012	5.3	.086	27
94	68	72	23	1	.003	350.	43.	4.9	9.7	-1.1	2.1	8.	-.006	3.8	.065	1
95	68	73	0	43	.113	346.	64.	7.3	10.2	2.4	1.1	8.	.005	3.1	.048	36
96	68	73	1	63	.166	351.	51.	5.5	10.1	2.5	-.2	8.	-.003	3.5	.058	60
97	68	73	2	22	.058	354.	41.	6.3	9.8	2.7	2.0	8.	-.011	3.2	.048	22
98	68	73	3	11	.029	354.	35.	6.1	9.3	1.9	1.6	8.	-.013	3.0	.046	11
99	68	73	4	1	.003	348.	25.	6.4	11.1	1.6	.6	7.	-.006	4.8	.041	1
100	68	73	5	4	.011	353.	25.	10.4	13.1	.4	-.5	8.	.004	1.8	.019	1
101	68	73	6	2	.005	333.	15.	8.4	10.2	1.6	2.4	7.	.000	.0	.000	0
102	68	73	7	8	.015	318.	21.	5.7	12.7	.8	-.5	7.	.015	3.1	.048	8
103	68	73	8	1	.001	336.	8.	2.9	8.3	1.1	-.5	7.	.014	6.4	.074	1
104	68	73	20	15	.096	337.	34.	21.6	20.9	2.4	1.0	6.	-.004	.9	.018	4
105	68	74	1	15	.040	331.	22.	20.3	24.2	3.7	5.2	7.	-.001	1.3	.023	9
106	68	74	2	280	.739	329.	18.	25.1	30.4	4.1	4.3	7.	.000	1.3	.029	5
107	68	74	3	240	.633	326.	18.	25.7	32.4	4.0	4.0	6.	.000	.0	.000	0
108	68	74	4	253	.668	328.	19.	28.8	38.8	4.9	4.3	6.	-.020	2.6	.033	2
109	68	74	5	222	.586	342.	29.	60.2	62.4	6.7	4.5	6.	-.031	2.2	.026	18
110	68	74	6	232	.612	347.	31.	82.1	76.5	7.5	3.6	7.	-.017	2.1	.023	23
111	68	74	7	253	.668	357.	35.	78.4	80.7	6.7	3.8	6.	-.008	1.7	.021	68
112	68	74	8	182	.480	373.	63.	57.1	60.8	5.2	1.6	6.	-.007	2.1	.028	96
113	68	74	9	45	.073	403.	160.	10.7	18.8	2.6	-1.5	4.	-.062	7.0	.073	10
114	68	74	10	11	.018	412.	149.	10.7	21.3	2.5	-.8	5.	-.069	3.7	.085	4
115	68	74	11	73	.145	408.	199.	10.5	20.2	3.0	-1.3	4.	-.060	6.1	.084	14
116	68	74	12	191	.504	410.	197.	13.4	21.2	3.3	.2	5.	-.031	5.6	.083	101